Journal of Crystal Growth 115 (1991) 542–550
North-Holland

JOURNAL OF CRYSTAL GROWTH

Invited paper

Vapour growth of silicon: growth anisotropy and adsorption

J.G.E. Gardeniers

Micromechanical Transducers Group, MESA Research Institute, University of Twente, P.O. Box 217, 7500 AE Enschede, Netherlands

and

L.J. Giling

Research Institute for Materials, Department of Experimental Solid State Physics 3, University of Nijmegen, Toernooiveld, 6525 ED Nijmegen, Netherlands

The development of facets on hemispherical single crystal substrates is investigated for growth in a near-equilibrium hot-wall CVD system, in order to study the orientation dependence of silicon crystal growth as a function of gas phase parameters in the Si–H–Cl system. It is found that only faces with indices {*hhk*} are stable. On the basis of their different behaviour as a function of experimental conditions, these faces are divided into $\{hhk\}_{h>k}$ and $\{hhk\}_{h<k}$ faces. The {111} and {001} faces have to be considered separately. From the experimental dependencies it is concluded that the adsorption of chlorine and hydrogen plays a dominant yet ambivalent role: it stabilizes the {001} and the $\{hhk\}_{h>k}$ faces, but destabilizes the $\{hhk\}_{h<k}$ faces. In order to explain these effects, it has to be assumed that under CVD conditions dimer-like reconstructions are present on all silicon faces. The interplay between surface dimer reconstructions and adsorption processes also shows up in the kinetic roughening of the different faces at high supersaturations. Theoretical calculations of the probabilities of adsorption of growth species on the different faces are used to explain the differences in kinetic roughening of these faces and the observed change in orientation of growth hillocks on the {111} faces which occurs when the supersaturation is increased.

1. Introduction

In this paper we shall give a review of an experimental study on epitaxial growth on hemispherical single crystal substrates as a function of gas phase parameters in a near-equilibrium hot-wall CVD system [1–4]. The experimental results will be interpreted on the basis of surface reconstruction models and theoretical calculations of the adsorption probabilities of gas phase species on the different faces, as reported earlier for the Si–H CVD system [5,6]. Some new insights are obtained from an extension of the adsorption calculations to the Si–H–Cl system.

2. Review of experimental results

The photograph in fig. 1a shows a representative example of a silicon hemisphere resulting after epitaxial silicon deposition with the Si–H–Cl CVD system. Fig. 1b shows a schematical drawing of the same hemisphere. These figures demonstrate the three main categories of growth features which can be found on practically all hemispheres after growth, viz.: (i) flat faces, i.e. parts of the hemisphere which are not curved in any direction, (ii) macroscopic steps, i.e. hemisphere parts which are curved in one direction, and (iii) parts of the hemisphere which are curved in all directions (the white regions in fig. 1b).

For all the growth conditions investigated in our work, features (i) and (ii) were only observed on parts of the hemispheres which correspond to the crystallographic ⟨110⟩ zones. Figs. 2a to 2d show representative photographs of some of the observed flat faces.

In table 1 all the experimentally observed flat faces are summarized. The crystallographic indices of the faces were derived from: (i) the angle

0022-0248/91/$03.50 © 1991 – Elsevier Science Publishers B.V. All rights reserved

of the face with the (111) face, which was measured with the aid of a goniometer (accuracy: ca. 0.1°; the (111) face can be identified easily because of its threefold-symmetric shape, see fig. 2c); (ii) the position and the frequency of occurrence of symmetry-related faces. It has to be mentioned that we never observed flat {112} faces, as reported by others [7,8], or flat faces with crystallographic indices {11*n*}, where $n > 3$ (like {115} [9]).

Table 2 gives a summary of our experimental results on the occurrence and appearance of the different faces as a function of CVD conditions. The observations which are the most remarkable, are:

(i) an increase in temperature has an opposite effect on the stability of the $\{hhk\}_{h>k}$ faces and the $\{hhk\}_{h<k}$ faces: the latter faces are only observed above a certain transition temperature, which depends on pressure and Cl–H ratio in the gas mixture, while the $\{hhk\}_{h>k}$ faces become less stable at the higher temperatures;

(ii) for growth at high temperatures it is observed that the growth hillocks on the {111} faces at low supersaturation are terminated by straight steps parallel to one of the ⟨110⟩ directions and moving in the $\langle \bar{1}\bar{1}2 \rangle$ directions, while at high supersaturations the growth hillocks become bound by straight steps moving in the $\langle 11\bar{2} \rangle$ directions (see fig. 3).

3. Theoretical aspects of the growth habit of silicon

In accordance with the CVD results of others [7,8,10,11], in our study only flat faces (or macrosteps) with crystallographic indices {*hhk*} were observed. A reason for this is the high stability of the ⟨110⟩ periodic bond chains (PBCs), which consist of nearest-neighbour covalent bonds only and which build up the silicon (or more general: the diamond-type) crystal bulk structure [12]. According to a (first-order) PBC analysis of the silicon crystal structure [12], however, only the {111} faces should be stable, flat faces. This is clearly in contradiction with experimental observations, from which it can be inferred that bulk-bonding (broken-bond) considerations alone do not give adequate descriptions of the surface structure of silicon during CVD. The reason for this is that at the surface certain (de) stabilizing

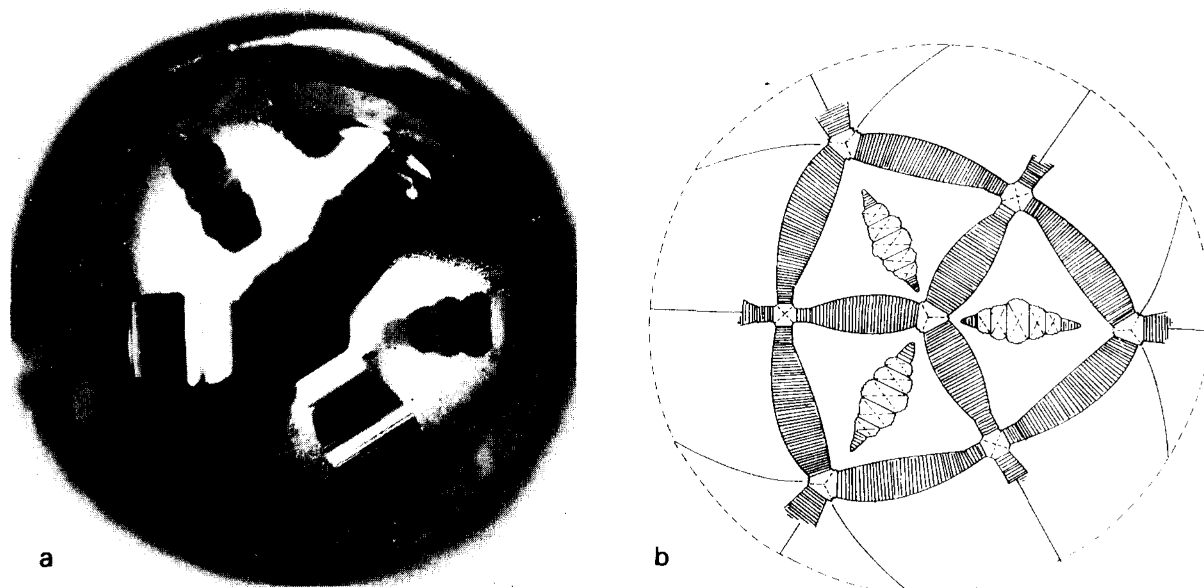

Fig. 1. (a) View on top of a hemisphere (diameter: 6 mm) after silicon deposition. (b) Schematical drawing of the hemisphere in (a).

interactions are present, which do not exist in the bulk of the crystal. In the case of silicon these are:
(a) reconstruction and relaxation processes;
(b) adsorption processes.

In the following sections we shall discuss the consequences of these two categories of processes for the crystal habit of silicon.

3.1. The crystal habit of silicon under vacuum conditions: reconstruction processes

In order to understand the crystal habit of silicon as a function of growth parameters on an atomic level, detailed knowledge of the structure of the different silicon faces is essential. Unfortunately, structural information on most of the silicon faces which are of interest to us (especially the high-index faces) is still lacking. Some general principles of surface stabilization can be derived from the studies reported up to now, though. The most important of these principles seem to be [14,15]:
(i) stabilization occurs mainly by minimization of the density of the so-called "dangling bonds" (DBs) on the surface, which can be accomplished by the formation of dimer bonds from two neighbouring DBs (as is the case on the Si (001)-(2 × 1) surface, see e.g. ref. [16]) or by adatoms over three adjacent DBs (like e.g. in the dimer-adatom-stacking fault (DAS), model of Si (111)-(7 × 7) [17]);
(ii) bond angle deviations away from the sp^3-hybridized optimum directions are less unfavourable than bond stretching; the latter causes too much stress in the surface layer if it becomes larger than about 5% [15]; these latter two processes can very well be described by the Stillinger–Weber [18] or related potential models [19].

In ref. [13] we have shown that, if principle (i) is applied to calculate the surface energies of $\{hhk\}$ faces, surface dimer formation will, besides for the {111} faces, which are already stable without any reconstruction, lead to very low surface energies for the {001} and the {113} faces also. Although theoretical calculations [20] show that our proposed structure for {113} is not very likely, our estimation of its surface energy is only slightly above that of Ranke's most stable dimer-reconstructed configuration [15], which confirms our prediction that in vacuum {113} is one of the most stable silicon faces because of the presence of surface dimers perpendicular to the ⟨110⟩ PBCs, so that stable two-dimensional "connected nets" [21] are obtained. Similar dimer reconstructions are likely to be present on all $\{hhk\}_{h<k}$ faces and might thus explain the high stability of these faces also.

Some experimental evidence seems to exist for the presence of dimer reconstructions on several other faces also, e.g. on {110} [22], where dimers on the edges of surface islands can lead to much lower surface energies than in the broken bond case [3], as is illustrated in figs. 4a and b. The DB density can be reduced by up to 50% by the presence of clusters with dimerized edges or even by 67% by the presence of adatoms which cover three DBs. However, the bonds in the smaller clusters or adatoms would have to be stretched substantially in order to obtain the required configurations, as is shown in fig. 4b. As bond stretching above 5% is very unfavourable, adatoms as shown in fig. 4a will not be very stable. The optimum cluster size will probably be in the region of 4 to 8 atoms, because the lower size islands will suffer from considerable bond angle strains, which were neglected in fig. 4b. Similar reasoning can be used to explain the high stability of the other $\{hhk\}_{h>k}$ faces. Detailed calculations of the surface energy of these faces should give more insight into this matter, but to our knowledge have not yet been performed.

3.2. The crystal habit of silicon under CVD conditions: adsorption processes

Although it is very hard to confirm experimentally, it is most likely that the above-mentioned principles will also apply to silicon surfaces exposed to CVD conditions. However, as (epitaxial) CVD processes usually are performed at high temperatures and high partial pressures of reactive species, it is questionable whether all the reconstructions observed in UHV studies can ex-

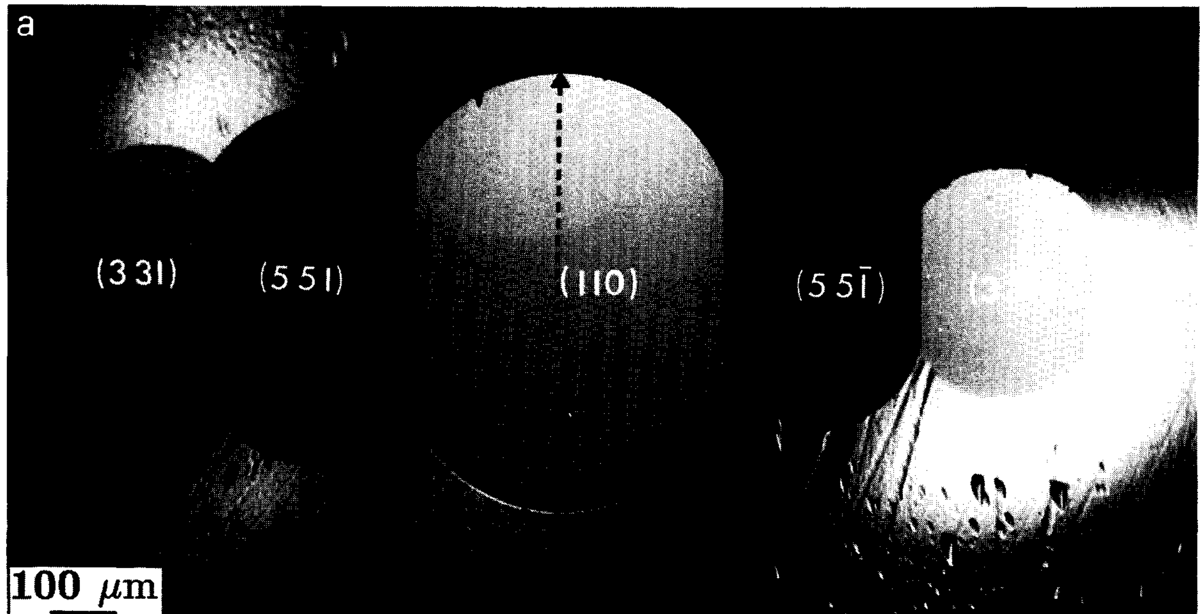

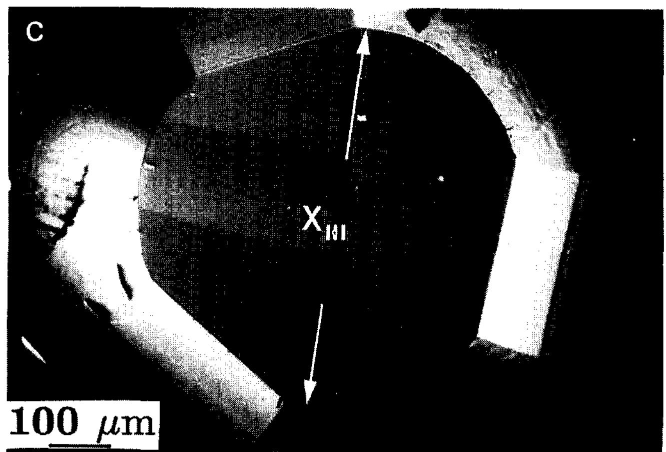

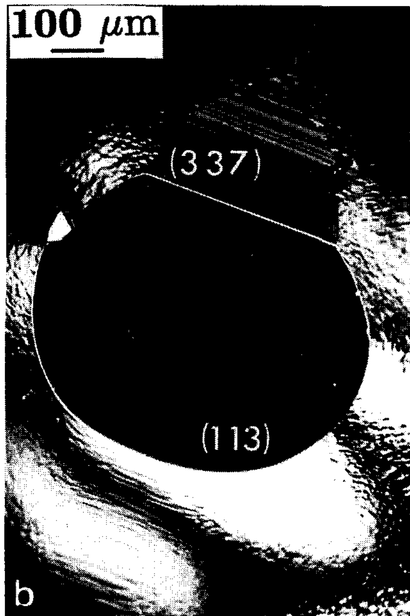

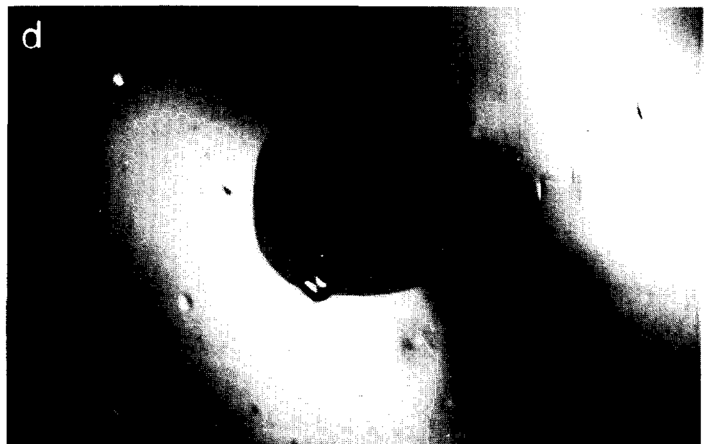

Fig. 2. Photographs of several faces as observed on hemispheres after silicon deposition. (a) the $\{hhk\}_{h>k}$ faces; (b) two of the $\{hhk\}_{h<k}$ faces, viz. {113} and {337}; (c) one of the {111} faces; (d) one of the {001} faces.

Table 1
Indices of the observed flat faces and their angles with the (111) face

Miller indices	Measured angle [a] (deg)	Theoretical angle (deg)
$11\bar{1}$	70.5 $\pm$0.1 (3)	70.53
001	−54.8 $\pm$0.1 (3)	−54.74
$\{hhk\}_{h>k}$ faces		
110	35.31$\pm$0.06 (3)	35.26
551	27.22$\pm$0.06 (6)	27.22
331	21.9 $\pm$0.1 (6)	22.00
$\{hhk\}_{h<k}$ faces		
113	−29.5 $\pm$0.1 (12)	−29.49
55 13	−26.1 $\pm$0.2 (4)	−26.19
337	−23.5 $\pm$0.1 (12)	−23.51
99 19	−20.86$\pm$0.08 (7)	−20.92
77 13	−17.45$\pm$0.08 (9)	−17.45
335	−14.3 $\pm$0.3 (2)	−14.42

[a] Averaged values from goniometer measurements of a certain number of different faces with the same indices on the same hemisphere. This number is placed in parentheses. The uncertainties mentioned in the column are the standard deviations from the average.

Table 2
Summary of experimental results

Faces	Near-equilibrium	High supersaturation
{111}, {110}	Flat faces; stability decreases with increasing temperature; no effect of Cl/H ratio or pressure	Flat faces at lower temperature; kinetic roughening at high temperatures
{001}	Flat faces; stability decreases at higher temperature, lower pressure or lower Cl/H ratio	Flat faces at lower temperature; stability decreases at higher temperature at which also kinetic roughening occurs
{331}, {551}	Flat faces; stability decreases at higher temperature, lower pressure or lower Cl/H ratio	Flat faces at lower temperature; not present at higher temperatures
$\{hhk\}_{h<k}$ [a]	Macrosteps at lower temperature; flat faces at higher temperatures; the transition from macrosteps to flat faces shifts to lower temperatures for lower pressures and/or lower Cl/H ratios	Similar to near-equilibrium results

[a] The temperature at which the transition from macroscopic steps to stable flat faces takes place, increases in the order: {113}, {337} < {77 13} < {99 19} < {55 13} < {335}.

ist under CVD conditions, because the surfaces will be covered by rather dense adsorption layers.

As experimental determination of adsorption layers is no sinecure and attempts in this direction have only occasionally been successful, a theoretical approach starting from the knowledge of the thermochemistry of the crystal growth system is very useful. In the field of semiconductor CVD up to now several theoretical analyses were reported [23–26], which all follow the following general lines of thought: (i) the partial pressures of likely adsorbates are calculated with the aid of known thermochemical data for specific conditions, with the assumption that some equilibrium situation exists; (ii) the adsorption sites on the surface are defined according to broken bond models of the crystal surface; (iii) adsorption thermochemical data are derived from known molecular properties of the constituents of the considered chemical system with the aid of partition functions; (iv) the surface coverage is calculated with the aid of the well-known Langmuir isotherm or modifications thereof.

According to these general lines, in refs. [5,6] the equilibrium coverage of Si (111), (001)-(1 × 1) and (001)-(2 × 1) surfaces was calculated. In these calculations the surface bond strengths of all possible adsorbates from the Si–H system were de-

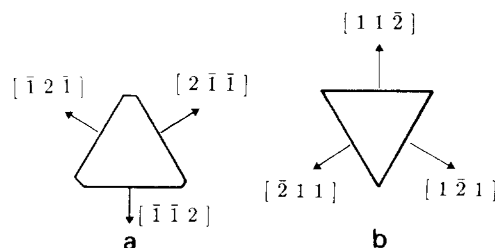

Fig. 3. Schematical drawings of directions of slowest step movement for growth hillocks on (111). (a) normally observed hillock shape (see also fig. 2c); (b) hillock shape for high temperature growth at high supersaturations (see also ref. [5]).

scribed with sums of two- and three-body interactions according to the Stillinger–Weber model [18,19], while as an extra important contribution to the bond strength of diradicals also the pairing energy was included. It was demonstrated that when the bond strengths are defined in this way, a consistent description of the bonds in gaseous silicon hydrides is provided, which indicates that the method should be applicable to the adsorption processes with acceptable accuracy.

In the present study we have extended the calculations to the Si–H–Cl system, using the adsorption thermochemical data of table 3, which were derived with the method described above with the aid of thermochemical and spectroscopic data from standard data tables [27]. In fig. 5 we show the result of calculations for a gas phase composition which is representative for our experimental conditions. In the calculations we have neglected the interactions which may exist between the adsorbates (see e.g. ref. [23]).

Similar to the previously reported results for the Si–H system, it is calculated that for low supersaturations in the Si–H–Cl system adsorption on Si (001)-(2 × 1) occurs on the atoms involved in the dimers, without the destruction of the dimer bonds. For these conditions adsorption on (001)-(2 × 1) and (111) is very much alike: the coverage with H and Cl is high on both surfaces, at all temperatures from 800 to 1600 K. On the other hand, the coverage with silicon species (i.e. growth species) is low, which can be interpreted in terms of the existence of a nucleation barrier on both faces, which again explains the observation of flat (111) and (001) faces in the growth experiments (fig. 2).

It is found in the calculations that at the higher supersaturations species, which have the ability to form two or four bonds with the surface atoms (especially Si_2), show a tendency to insert into the dimer bonds on (001)-(2 × 1). Thus, under these conditions growth readily proceeds on the (001) face. The layer growth of the face nevertheless remains, as the insertion of Si_2 species into dimer bonds does not lead to extra nucleation sites on the surface. This model explains the presence of smaller, but clearly observable (001) facets on the hemispheres at the higher supersaturations (table 2). As according to the discussion in the foregoing section the $\{hhk\}_{h<k}$

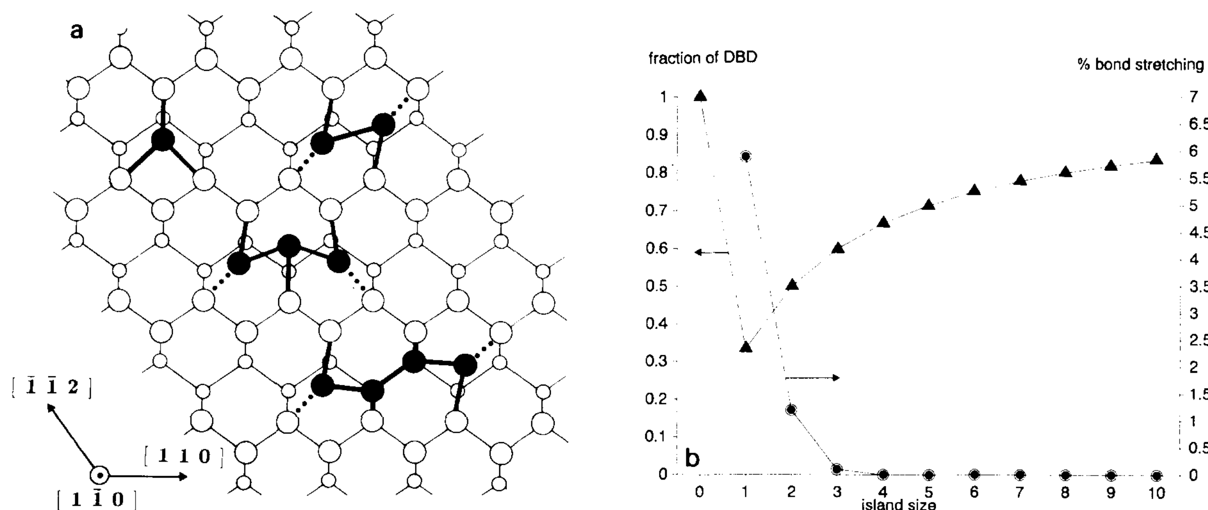

Fig. 4. (a) The most likely (i.e. with minimal bond stretching) configurations of adatoms and islands containing 2, 3 or 4 atoms on the (110) surface. Closed circles: adatoms or cluster atoms; large open circles: surface atoms; small open circles: subsurface atoms; dotted lines: dimer bonds. (b) Calculated fractions of the dangling bond density which remains after the addition of adatoms or islands on (110) and the mean percentage of bond stretching in the surface bonds of the adatoms or islands (neglecting bond angle deviations) as a function of island size.

Table 3
Adsorption thermodynamical data for the Si–H–Cl system

(a) Adsorption on Si {111} at 298 K [a)]

Species	ΔH^0_{ads} (kJ mol^{-1})	ΔS^0_{ads} (J mol^{-1} K^{-1})
Cl	−413	−139
SiCl	−241	−149
$SiCl_2$	−110	−207
$SiCl_3$	−281	−250
SiHCl	−178	−181

(b) Adsorption on Si (001)-(2×1) at 298 K [a)]

Species [b)]	ΔH^0_{ads} (kJ mol^{-1})	ΔS^0_{ads} (J mol^{-1} K^{-1})
Cl	−413	−139
μ^1-SiCl	−241	−149
μ^2-SiCl	−122	−182
μ^1-$SiCl_2$	−110	−207
μ^2-$SiCl_2$	−207	−263
$SiCl_3$	−281	−250
μ^1-SiHCl	−178	−181
μ^2-SiHCl	−274	−232

(c) Parameters required in the estimation of adsorption enthalpies [a),c)]

h_{SiCl}	353 kJ mol^{-1}
h_{SiSiCl}	20 kJ mol^{-1}
h_{HSiCl}	37 kJ mol^{-1}
h_{ClSiCl}	35 kJ mol^{-1}
P_{SiCl_2}	−150 kJ mol^{-1}
P_{SiHCl}	−83 kJ mol^{-1}
P_{SiCl}	−195 kJ mol^{-1}

[a)] For data of Si–H species: see ref. [6].
[b)] μ^2-species on Si (001)-(2×1) adsorb into dimer bonds [5,6].
[c)] h_{XY}: two-body interaction between atoms X and Y; h_{XYZ}: three-body interaction between atoms X, Y and Z, in which atom Y is the central atom; $P_{species}$: pairing energy of species [6].

faces contain dimers similar to those on (001), also on these faces no extra nucleation sites are created, so that growth will remain epitaxial up to high supersaturations.

On the other hand, on the (111) face at higher supersaturation the very high coverage with Si_2 species will lead to kinetical roughening, because these species during adsorption on this face are not in lattice positions. Under a continuous flux of growth species to the surface this will lead to extra nucleation sites and defective growth.

Concerning the orientation of the growth hillocks on (111) (fig. 3), it may be clear that the coverage of the steps with silicon species will increase at higher supersaturations. Also here the insertion of silicon species into dimer bonds plays an important role: as was discussed in ref. [28], growth hillocks on (111) are always bound by steps parallel to the $\langle 1\bar{1}0\rangle$ PBCs. Of these steps the ones moving into the $\langle 11\bar{2}\rangle$ directions have dimer-reconstructed edges, while steps moving into the opposite $\langle \bar{1}\bar{1}2\rangle$ directions have not. At low supersaturation the former steps move slower than the latter because of their higher stability, resulting in growth hillocks bound by $\langle \bar{1}\bar{1}2\rangle$ steps. However, at the higher supersaturations the insertion of growth species into these dimer reconstructed steps, just like on (001)-(2×1), becomes

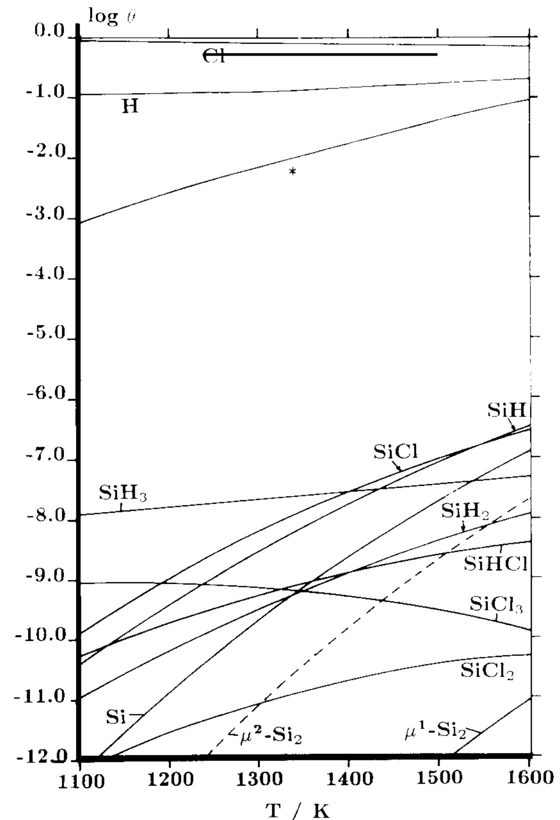

Fig. 5. Surface coverage, θ, of Si (111) and (001)-(2×1) for the Si–H–Cl CVD system as a function of temperature for the near-equilibrium gas phase input mixture of 3% SiH_2Cl_2, 6% HCl and 91% H_2. μ_1 and μ_2 are used to distinguish adsorbate configurations with one and two bonds to the surface, respectively. (*) is the fraction of empty surface sites.

so high, that these steps become the fastest moving, leading to hillocks bound by steps of the other stable kind, i.e. $\langle 11\bar{2} \rangle$ steps. This behaviour is exactly what was observed in the growth experiments (fig. 3; see also ref. [29]), and also explains the kinetical roughening of the $\{hhk\}_{h>k}$ faces, because the terraces with dimer-reconstructed edges, which these faces require to become stable (fig. 4), tend to disappear at the higher supersaturations.

Finally, the adsorption calculations can be used to explain the most remarkable observation that the {113} faces are stable only above a certain critical temperature, T_{cr}, which depends on the Cl/H ratio in the gas phase and on the pressure (see table 2); below this critical temperature macroscopic steps parallel to one of the $\langle 110 \rangle$ directions were observed in positions on the hemispheres corresponding to {113}. Similar results were found for the other $\{hhk\}_{h<k}$ faces, where each of the faces has its own critical temperature (see the note below table 2). An explanation for this observation is the destabilization of certain faces due to the adsorption of species which lower the step free energy [6,13] on the faces(in refs.[2,4] we called this phenomenon "chemical roughening", to distinguish it from the well-known kinetical and thermal roughening of faces). In the case of the $\{hhk\}_{h<k}$ faces this effect is caused by the simultaneous adsorption of Cl and H; the faces thus become more stable for conditions at which the coverage of these species (especially that of Cl [4]) is lower, viz. at lower Cl/H ratios, higher temperatures (fig. 5) and lower pressures. In contrast to this, we observed stabilization of the {001} and the $\{hhk\}_{h>k}$ faces (table 2) at conditions where the coverage with Cl is expected to be higher. Although the exact mechanism leading to this stabilization is not known, it is suggested that the stabilization of the $\{hhk\}_{h>k}$ faces occurs indirectly via a mechanism which favours the formation of dimer stabilized terraces on these faces (fig. 4).

4. Summary

The orientation dependence of silicon crystal growth with the Si–H–Cl CVD system as a function of temperature, pressure and Cl/H ratio in the gas phase was studied with the aid of hemispherical single crystal specimens. It was concluded that the main factors governing the stability of silicon faces are: (i) the presence of $\langle 110 \rangle$ PBCs (which are entities of the bulk crystal structure of Si); (ii) dimerlike reconstructions; (iii) the adsorption of Cl and H, which leads to either stabilization (as was observed for the {001} and the $\{hhk\}_{h>k}$ faces) or destabilization (as was observed for the $\{hhk\}_{h<k}$ faces at lower temperatures, higher Cl/H ratios and higher pressures).

The observed high supersaturation effects, i.e. the change in orientation of the growth hillocks on (111) and the kinetical roughening of the different faces, were interpreted in terms of the different adsorption probabilities and configurations of growth species on the different steps and faces.

References

[1] J.G.E. Gardeniers, W.E.J.R. Maas, R.Z.C. van Meerten and L.J. Giling, J. Crystal Growth 96 (1989) 821.
[2] J.G.E. Gardeniers, C.H. Klein Douwel and L.J. Giling, J. Crystal Growth 108 (1991) 319.
[3] J.G.E. Gardeniers, M.M.W. Mooren and L.J. Giling, Surface Sci. 236 (1990) 85.
[4] J.G.E. Gardeniers, M.M.W. Mooren, M.H.J.M. de Croon and L.J. Giling, J. Crystal Growth 102 (1990) 233.
[5] J.G.E. Gardeniers, F. de Jong and L.J. Giling, Surface Sci. 233 (1990) 123.
[6] J.G.E. Gardeniers, L.J. Giling, F. de Jong and J.P. van der Eerden, J. Crystal Growth 104 (1990) 727.
[7] J. Nishizawa, T. Terasaki and M. Shimbo, J. Crystal Growth 13/14 (1972) 297.
[8] C.H.J. van den Brekel, J. Crystal Growth 23 (1974) 259.
[9] W. Ranke and Y.R. Xing, Phys. Rev. B 31 (1985) 2246.
[10] S. Mendelson, J. Appl. Phys. 35 (1964) 1570.
[11] S.K. Tung, J. Electrochem. Soc. 112 (1965) 436.
[12] P. Hartman, Z. Krist. 121 (1965) 78.
[13] J.G.E. Gardeniers, W.E.J.R. Maas, R.Z.C. van Meerten and L.J. Giling, J. Crystal Growth 96 (1989) 832.
[14] K.C. Pandey, Physica B 117/118 (1981) 761.
[15] W. Ranke, Phys. Rev. B 41 (1990) 5243.
[16] R.J. Hamers, R.M. Tromp and J.E. Demuth, Phys. Rev. B 34 (1986) 5343.
[17] K. Takayanagi, Y. Tanishiro, M. Takahashi and S. Takahashi, Surface Sci. 164 (1985) 367.
[18] F.H. Stillinger and T.A. Weber, Phys. Rev. B 31 (1985) 5262.
[19] J.P. van der Eerden, Liu Guang-Zhao, F. de Jong and M.J. Anders, J. Crystal Growth 99 (1990) 106.

[20] D.J. Chadi, Phys. Rev. B 29 (1984) 785.
[21] P. Bennema and J.P. van de Eerden, in: Morpholoy of Crystals Ed. I. Sunagawa (Terrapub, Tokyo, 1987) p. 1.
[22] H. Ampo, S. Miura, K. Kato, Y. Ohkawa and A. Tamura, Phys. Rev. B 34 (1986) 2329.
[23] A.A. Chernov and M.P. Rusaikin, J. Crystal Growth 52 (1981) 185.
[24] R. Cadoret, in: Current Topics in Materials Science, Vol. 5, Ed. E. Kaldis (North-Holland, Amsterdam, 1980) p. 219.
[25] J. Korec and M. Heyen, J. Crystal Growth 60 (1982) 297.
[26] L.J. Giling, H.H.C. de Moor, W.P.H.J. Jacobs and A.A. Saaman, J. Crystal Growth 78 (1986) 303.
[27] JANAF Thermochemical Tables, J. Phys. Chem. Ref. Data 11 (1982) Supplement, p. 695.
[28] W.J.P. van Enckevort and L.J. Giling, J. Crystal Growth 45 (1978) 90.
[29] J. Nishizawa and M. Shimbo, J. Crystal Growth 24/25 (1974) 215.